Tellus SERIES B CHEMICAL AND PHYSICAL METEOROLOGY
PUBLISHED BY THE INTERNATIONAL METEOROLOGICAL INSTITUTE IN STOCKHOLM

Tellus (2011), 63B, 1026–1039

TELLUS

Effects of black carbon aging on air quality predictions and direct radiative forcing estimation

By S.H. PARK[1], S.L. GONG[2]*, V.S. BOUCHET[2], W. GONG[2], P.A. MAKAR[2], M.D. MORAN[2], C.A. STROUD[2] and J. ZHANG [2], [1]*Department of Environmental Engineering, Sunchon National University 315 Maegok-dong, Suncheon, Jeonnam 540–742, South Korea;* [2]*Air Quality Research Division, Science and Technology Branch, Environment Canada 4905 Dufferin Street, Toronto, Ontario M3H 5T4, Canada*

(Manuscript received 9 September 2009; in final form 27 May 2011)

ABSTRACT

An aging scheme for black carbon (BC) aerosol was implemented into a regional air-quality forecast model to study the impact of BC aging on air quality predictions. Three different assumptions for the mixing state of BC—external mixture, internal mixture and gradual aging—were used to simulate the distribution of BC particles over North America in April 2002. Cloud –condensation nuclei number and BC wet deposition rate increased significantly and BC mass column loading decreased as a result of BC aging. With the gradual aging process incorporated into the model, the comparison of ground level BC concentration predictions with surface observations was slightly improved. Estimation of the average direct radiative forcing of BC over the spatial domain of this study showed that the factor of direct forcing enhancement by BC aging was much smaller than the mixing state effect factor. The effect of increased wet deposition due to aging compensated partially for the effect of increased absorbance suggesting that the change in the hygroscopic properties of BC due to aging must be taken into account to quantify accurately the effect of BC aging on climate.

1. Introduction

Black carbon (BC) refers to a strongly light-absorbing carbonaceous atmospheric aerosol component (Bond and Bergstrom, 2006). BC is one of the chemical components causing the large uncertainty in recent estimates of the climate impact of aerosol particles (IPCC, 2007). BC absorbs visible sunlight and heats the atmosphere (Ech et al., 1998; Satheesh and Ramanathan, 2000), whereas light-scattering components such as sulphate cools the earth–atmosphere system. One can refer to Ramanathan and Carmichael (2008) for a detailed review on the climate effect of atmospheric BC. The climate impact of BC depends on the optical properties and hygroscopicity of BC-containing aerosol particles, which are determined in part by their state of mixing with other particle species. According to computations based on Mie theory, an internally mixed aerosol exerts much stronger absorbance than an externally mixed one with the same size, shape and chemical composition (Ackerman and Toon, 1981; Martins et al., 1998; Haywood and Boucher, 2000; Jacobson, 2001; Lesins et al., 2002).

Aging is the process that transforms hydrophobic, externally mixed BC particles into hygroscopic, internally mixed ones. Aging of BC particles takes place through interactions with other aerosol species: for example, condensation of sulphuric acid vapour onto the surface of BC particles, coagulation with soluble aerosol particles and heterogeneous oxidation occurring at the BC particle surface. Aging of BC particles not only affects climate through radiative effects but also influences air quality (AQ) because the increase in hygroscopicity results in an increase in the wet deposition rate and, consequently, a decrease in the lifetime of BC-containing particles, which are known to be carcinogenic (Dasenbrock et al., 1996). Therefore, information concerning the fate of BC aerosol particles from emission through transport and aging to removal is needed to assess quantitatively the impacts of BC on both climate and AQ.

Although the impact of aging and hence the mixing state of BC aerosol particles on climate has already been intensively investigated (Ackerman et al., 2000; Jacobson, 2000; Jacobson, 2001; Menon et al., 2002; Liu et al., 2005), there are relatively few studies in the literature on their influence on regional AQ. Croft et al. (2005) used a global climate model to simulate the impact of aging on removal rate and lifetime of BC aerosol particles. Due to computational limitations, however, they used

*Corresponding author:
Air Quality Research Division, Science and Technology Branch, Environment Canada, 4905 Dufferin Street, Toronto, Ontario M3H 5T4, Canada.
e-mail: Sunling.Gong@ec.gc.ca
DOI: 10.1111/j.1600-0889.2011.00558.x

a parameterization for the aging process instead of direct simulation. Zaveri et al. (2009) investigated the effects of mixing state assumptions on optical and CCN properties in an on-line regional forecast model and aerosol modules developed by Riemer et al. (2009), noting that mean optical properties of the aerosol were still sensitive to the mixing state after 2 days of aging, but that the sensitivity decreases with time. Riemer et al. (2010) also used the aerosol model of Riemer et al. (2009) to estimate the aging time scales of BC contained in an urban plume. Vogel et al. (2009) used the COSMO-ART with a modal structure designed to resolve the mixing state of BC to examine the impact of the aerosols on clouds and radiative properties within the COSMO weather forecast model, finding surface temperature changes in the 0.1–0.3 °C range, and a significant change in the precipitation pattern. Oshima et al. (2009) used a new two-dimensional aerosol representation following the method of Jacobson (2001), in which aerosol population was given for particle size and BC mass fraction, to resolve the mixing state of BC particles. This aerosol module was incorporated into a box model to simulate the aging of BC particles within a polluted plume. Jacobson (1997) and Jacobson et al. (2007) accounted for the aging of BC in simulating the aerosol effect on regional AQ and climate in southern California region. In those studies, however, sensitivity test to isolate the effect of BC aging was not performed: comparison between the simulations with and without aging process taken into account was not carried out. Vignati et al. (2010) compared two different BC aging schemes employed in a global chemical transport model (CTM): a simple approach considering only total BC mass with a constant wet removal rate and a microphysical aging scheme based on aerosol dynamics. They showed that the simple approach can lead to entirely wrong estimates on BC concentration over remote areas.

In this study, Environment Canada's (EC) regional AQ model AURAMS (A Unified Regional Air-quality Modelling System), was modified so that BC aging could be taken into account in its aerosol dynamics module. The modified model was then used to perform three simulations of the distribution of BC aerosol in North America in April 2002. This paper reports the results of the sensitivity analyses looking into how cloud condensation nuclei (CCN) concentration, BC concentration and BC wet deposition rate and lifetime are affected by BC particle aging. Based on these results, the impact of BC aging on regional AQ and on climate are then discussed.

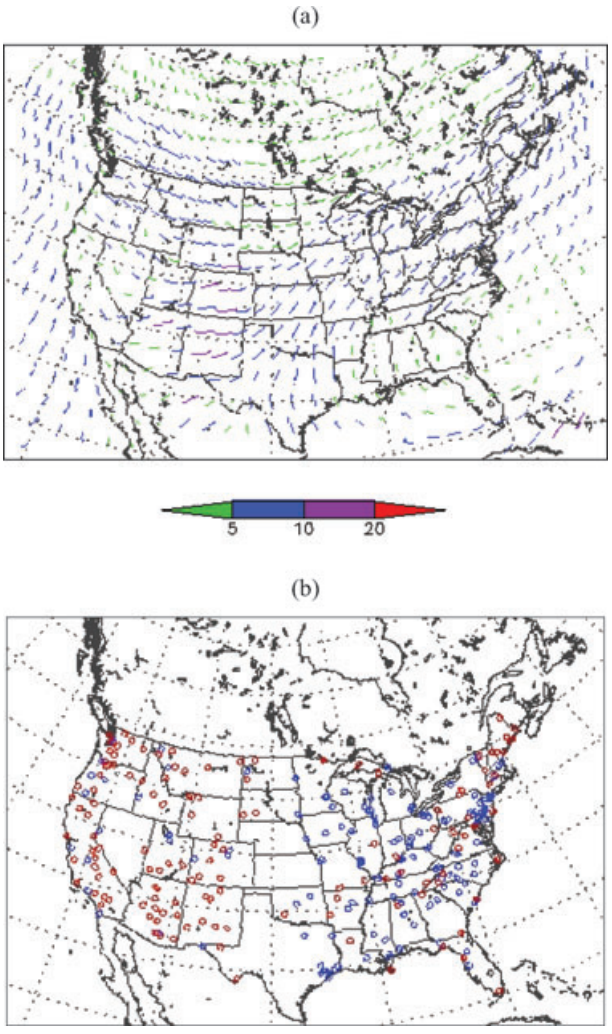

Fig. 1. The AURAMS CTM domain with (a) average horizontal wind field (m s^{-1}) 1 km above ground level during the April 2002 simulation period and (b) locations of the 130 IMPROVE (blue) and 147 STN (red) speciated $PM_{2.5}$ measurement stations. Wind barbs are plotted every second degree longitude and latitude.

2. Model description, configuration and aging parameterization

An off-line, size- and composition-resolved atmospheric particulate-matter (PM) modelling system, AURAMS, which consists of the AURAMS CTM and its accompanying meteorological driver, Global Environmental Multiscale model (GEM), was used in this study to simulate the physics and dynamics of BC aerosol particles, including emission, transport and diffusion, coagulation, condensation, aging, hygroscopic growth, wet and dry removal and aerosol activation. The regional configuration of GEM version 3.2.0 used for this study employed a horizontal grid size of 0.22° (∼24 km) on a rotated latitude–longitude grid. Meteorological fields required by the AURAMS CTM version 1.3.1 were stored at every CTM advection time step (900 s). The grid selected in this study for the CTM was the 42-km 150 × 106 horizontal grid on a secant polar stereographic projection true at 60°N shown in Fig. 1. The 28 unevenly spaced vertical levels ranged from the surface to 25 km above ground level (AGL), with 14 levels located in the first 2 km.

A sectional approach was used to represent the PM size distribution; the 12 size bins were logarithmically spaced and ranged from 0.01 to 41 μm in particle diameter. The lower size limit

of 10 nm may cause some error when homogeneous nucleation is the major aerosol source. Nevertheless, this is not expected to hinder the purpose of this study, simulating the effect of BC particles, because the fresh BC particles are usually larger than 10 nm. Nine chemical components were considered to contribute to total aerosol mass: sulphate; nitrate; ammonium; sea-salt; BC; primary organic carbon; secondary organic carbon; crustal material and particle-bound water, among which sulphate, nitrate, ammonium and sea-salt were assumed to be soluble for the purpose of BC aging due to coagulation. The partial solubility of secondary organic carbon was not accounted for the simplicity. Equilibrium between soluble species and aerosol water was assumed based on the Kohler equation. Both in-cloud and below-cloud scavengings are accounted for in wet deposition process. In-cloud production of secondary aerosol species, for example, sulphate, is also accounted for. Refer to Gong et al. (2006) for detailed information on the representation of wet deposition including cloud processing of gases and aerosols in AURAMS. For dry deposition of gaseous and particulate species, one can refer to Zhang et al. (2001) and (2002), respectively.

The condensation rate that defines the consumption rate of two condensable gas-phase species (sulphuric acid vapour and condensable organic gas) and the corresponding growth rate of aerosol particles is calculated using a modified Fuchs-Sutugin equation (Fuchs and Sutugin, 1971). To calculate the change in particle size distribution due to coagulation, a semiimplicit numerical solution is used (Jacobson et al., 1994). Zero-gradient chemical lateral boundary conditions were applied for all gas and particle species (Samaali et al., 2009). Refer to Park et al. (2007) and the references therein for more detailed information on GEM and the AURAMS CTM.

Emissions were obtained from the 2000 Canadian national criteria air contaminant (CAC) emission inventory (http://www.ec.gc.ca/inrp-npri) and the 2001 U.S. and 1999 Mexican national CAC inventories (http://www.epa.gov/ttn/chief). Gridded hourly emissions files were prepared using version 2.1 of SMOKE (Sparse Matrix Operator Kernel Emissions Modelling System) (see http://cf.unc.edu/cep/empd/products/smoke/index.cfm). Due to their sporadic and intermittent nature, estimates of wildfire and prescribed burning emissions from the annual national inventories were not used because they could not be gridded and time-stamped properly.

2.1. Parameterization of BC aging

In the current version of AURAMS, all of the PM chemical components are assumed to be internally mixed in each size section or bin. That is, no distinction is made between particles that have just been emitted versus those that have been present in the atmosphere for some time. All particles of the same size that are contained in the same model grid cell are assumed to have the same chemical composition, but chemical composition can vary between different size bins in the same grid cell and between the same size bins in adjacent grid cells. This model version is referred to as INTMIX version, in which all BC is aged, hereafter.

In order to evaluate the effect of the BC aging process, however, the treatment of particle mixing state had to be changed. In one revised version of AURAMS employed in this study for comparison purposes, newly emitted BC particles are assumed to be externally mixed initially and to remain externally mixed (that is, they were not allowed to participate in coagulation with internally mixed particles, and were not used as seeds for condensation, in order to test the sensitivity of the system to the mixing state). This model version is called the EXTMIX version, in which BC is never aged. In a second revised version, both the condensation of sulphuric acid vapour onto BC particles and the coagulation of BC particles with pre-existing internally mixed particles is assumed to 'age' these particles and convert them to the internally mixed state. To embody this aging algorithm, an extra set of 12 bins was added for the externally mixed BC particles. This model version is called the AGING version, in which some BC is aged and some is not, hereafter. Note that aging by heterogeneous oxidation on particle surfaces is neglected in this study because the contribution of heterogeneous oxidation to BC aging is, in spite of its high uncertainty, expected to be much less significant than that of condensation and coagulation (Saathoff et al., 2003; Croft et al., 2005). Note too that only internally mixed particles are subject to hygroscopic growth (particle 'swelling'), so the corresponding equilibrium wet radius is only calculated for them. The equilibrium-wet radius is used in turn in calculations of coagulation, dry deposition and gravitational settling.

In the AGING version, it is assumed that an externally mixed particle has aged long enough to become internally mixed when it acquires a sufficient amount of soluble material to shift the particle hygroscopicity from hydrophobic to hydrophilic. For aging by condensation, a single-layer (i.e. one-molecule thick) coating of the externally mixed particle by sulphate is used as the criterion for completion of aging following the approach of Vignati et al. (2004). There is some evidence that condensing organic gases can have the same effect (Martins et al., 1998; Croft et al., 2005) but this process has not been considered in this study. Let x_i be the mass fraction (i.e. mass mixing ratio) of externally mixed BC particles in size section i, $Q_{\mathrm{cond},i}$ be the condensational mass flow rate of sulphate onto a single externally mixed BC particle in section i (kg s^{-1}) and S_i be the threshold mass of sulphate required to coat that BC particle completely (kg). Then, the rate of aging can be expressed by

$$\frac{1}{x_i}\frac{\mathrm{d}x_i}{\mathrm{d}t} = -\frac{Q_{\mathrm{cond},i}}{S_i}. \quad (1)$$

$Q_{\mathrm{cond},i}$ is calculated in AURAMS using a modified Fuchs-Sutugin equation (Fuchs and Sutugin, 1971). Under the single-layer aging assumption, a simple approximation for S_i, as a uniform spherical shell with the thickness of a single sulphate

molecule, is expressed as

$$S_i = \pi d_{p,i}^2 d_{\mathrm{SO_4}} \rho_{\mathrm{SO_4}}, \tag{2}$$

where $d_{p,i}$ is the particle diameter in section i, and $d_{\mathrm{SO_4}}$ and $\rho_{\mathrm{SO_4}}$ are the diameter of a sulphate molecule and the density of particle sulphate, respectively. $d_{\mathrm{SO_4}}$ can be related to $\rho_{\mathrm{SO_4}}$ by the following equation expressing the equivalence of macroscopic and microscopic expressions for the mass of a single sulphate molecule:

$$\rho_{\mathrm{SO_4}} d_{\mathrm{SO_4}}^3 = \frac{M_{\mathrm{SO_4}}}{N_{\mathrm{A}}}, \tag{3}$$

where $M_{\mathrm{SO_4}}$ is the molecular mass of sulphate and N_{A} is Avogadro's number. Combining Eqs (1)–(3), we have the following equation for the rate of aging by condensation:

$$\frac{1}{x_i}\frac{\mathrm{d}x_i}{\mathrm{d}t} = -\frac{Q_{\mathrm{cond},i}}{\pi d_{p,i}^2 \left(\frac{M_{\mathrm{SO_4}} \rho_{\mathrm{SO_4}}^2}{N_{\mathrm{A}}}\right)^{1/3}}. \tag{4}$$

The above-shown formulation is based on the assumption that all BC particles are spherical. In reality, however, BC particles are often aggregates that have larger surface area than spherical counterparts with the same volume. Thus, it must be kept in mind that eq. (4) may overestimate the rate of aging due to condensation. If the aggregate structure is destroyed due to restructuring during aging, the error may not be very large.

Aging by coagulation is taken into account similarly, but with a different criterion for the completion of aging. During coagulation, an externally mixed BC particle is not 'coated' by soluble species but instead collides with other particles that contain soluble species. Thus, an externally mixed particle is assumed to be aged by coagulation when it acquires soluble material (sulphate, nitrate, ammonium and sea-salt) of more than 5% of its mass following the approach of Jacobson (2001). The 5% mass criterion is equivalent to the single-layer sulphate criterion for a 36-nm spherical BC particle. For a larger particle, 5% mass is greater than the mass of single-layer sulphate, while the opposite is the case for a smaller particle. When an externally mixed particle collides with an internally mixed particle whose soluble mass is greater than 5% of the insoluble mass of the resulting particle, it is converted into an internally mixed particle. If the internally mixed particle that collides with the externally mixed particle is so small that its soluble mass is less than 5% of the insoluble mass of resulting particle, the rate of aging by coagulation can be expressed, similarly to the case of aging by condensation, as

$$\frac{1}{x_i}\frac{\mathrm{d}x_i}{\mathrm{d}t} = -\frac{Q_{\mathrm{coag},i}}{S_i}, \tag{5}$$

where $Q_{\mathrm{coag},i}$ is the mass flow rate of soluble material onto a single externally mixed BC particle in section i by coagulation (kg s^{-1}) and S_i is the threshold mass of soluble material required to age that particle (kg), that is, 5% of the resulting particle mass. $Q_{\mathrm{coag},i}$ can be computed from the expression

$$Q_{\mathrm{coag},i} = \sum_k \beta_{ik} N_{\mathrm{int},k} m_{\mathrm{sol},k} = \sum_k \beta_{ik} x_{\mathrm{sol},k} \rho_a, \tag{6}$$

where β_{ik} is the coagulation kernel between an externally mixed BC particle in section i and an internally mixed particle in section k (m^{3}s^{-1}), $N_{\mathrm{int},k}$ is the number concentration of internally mixed particles in section k (m^{-3}), $m_{\mathrm{sol},k}$ is the mass of soluble material in a single internally-mixed particle in section k (kg), $x_{\mathrm{sol},k}$ is the mass fraction of soluble particulate species in section k and ρ_a is the air density (kg m^{-3}).

The amount of BC particles converted from externally mixed state to internally mixed state during a time step can now be obtained by integrating Eqs (4) and (5) assuming that the right-hand-side term is constant.

3. Results and discussion

The results of 1-month AURAMS simulations for April 2002 for each of the EXTMIX, AGING and INTMIX model versions are presented in this section. Each simulation covers the 29-day period from 0600 UTC, 1 April to 0600 UTC, 30 April 2002. GEM was run in 30-h segments beginning at 0000 UTC on each day and starting from objectively analysed fields produced by the Canadian Meteorological Centre of EC. The first 6 h of each GEM simulation were treated as spin-up time and only fields for the remaining 24 h were supplied to the AURAMS CTM. The first two days of the AURAMS CTM run were treated as a spin-up period to allow emissions and atmospheric concentrations to approach equilibrium.

As discussed in the Introduction, the direct consequence of BC aging is the change in particle mixing state, which has a number of implications on meteorology, AQ and climate. In this section, the impacts of BC aging processes and mixing-state changes on CCN activity, BC wet deposition, BC mass column loading and ground-level concentration of BC particles, predicted by model simulations are presented and discussed.

The average horizontal wind vector field at 1 km AGL predicted by GEM during the simulation period is shown in Fig. 1a. Westerly winds were generally dominant over the whole North American continent, which is a characteristic of the spring season.

3.1. *Impact of BC aging on surface BC concentration predictions*

In order to evaluate the model predictions of BC and to see how much the model prediction is affected by the incorporation of BC aging processes, the concentration of BC contained in ground-level $PM_{2.5}$ ($BC_{2.5}$ hereafter) predicted by the INTMIX and AGING model versions were compared to

Table 1. Performance statistics of $BC_{2.5}$ predicted by INTMIX and AGING model versions. M and O represent modelled and observed values, respectively.

Total number of data records	1940	
	INTMIX	AGING
Mean fractional bias $\left(= \frac{1}{N}\sum_{i=1}^{N}\frac{M_i - O_i}{(M_i+O_i)/2}\right)$	−0.10	−0.093
Mean fractional error $\left(= \frac{1}{N}\sum_{i=1}^{N}\frac{\lvert M_i - O_i\rvert}{(M_i+O_i)/2}\right)$	0.11	0.099
Agreement index $\left(= 1 - \frac{\sum_{i=1}^{N}(M_i - O_i)^2}{\sum_{i=1}^{N}(\lvert M_i - \bar{O}\rvert + \lvert O_i - \bar{O}\rvert)^2}\right)$	0.68	0.69

available observations. All of the observation data for surface BC aerosol concentrations used for model evaluation in this section were obtained from the EC National Atmospheric Chemistry (NAtChem) database (http://www.msc.ec.gc.ca/natchem). Among its data-contributing agencies/organizations, the U.S. Interagency Monitoring of Protected Visual Environments (IMPROVE) $PM_{2.5}$ speciation network and the U.S. Environmental Protection Agency (EPA) Air Quality System (AQS) Speciated Trends Network (STN) provide daily $BC_{2.5}$ concentrations obtained from 1-in-3 day 24-h sampling (Malm et al., 1994; Chu, 2004; Gego et al., 2005; Phillips and Finkelstein, 2006). The locations of the measurement stations of these two networks are shown in Fig. 1b. Different methods are used for determining $BC_{2.5}$ concentrations by the two networks: thermal/optical transmittance (TOT) by STN and thermal/optical reflectance (TOR) by IMPROVE. It was reported that TOT generally yields less BC amount by 30% than TOR with the same temperature protocol (Chow et al., 2004).

Figure 2a compares daily $BC_{2.5}$ (μg m^{-3}) concentrations predicted by the INTMIX model version with daily IMPROVE and STN network observations for April 2002. 130 IMPROVE stations and 147 STN stations reported valid measurements during this period. On average, INTMIX significantly underestimated the ground-level BC concentrations. With aging incorporated into the model (Fig. 2b), the comparison with observations was slightly improved: the linear regression slope changed from 0.32 to 0.35. Table 1 shows another performance statistic, the agreement index, of the two model versions. Considering disparate values over a span of about three orders of magnitude, the logarithms of $BC_{2.5}$ values were used here. Although the differences are not very large, AGING model version showed smaller bias and error and larger agreement index than INTMIX model version. In order to see if this difference is statistically significant, Z test (Devore, 1982) was performed. INTMIX-predicted $BC_{2.5}$/observed $BC_{2.5}$ was taken as one sample and AGING-predicted $BC_{2.5}$/observed $BC_{2.5}$ was taken as the other. The Z value was 1.87, smaller than the criterion value of 1.96, indicating that the difference between the two samples is not statistically significant. Figure 2c shows an intermodel comparison between

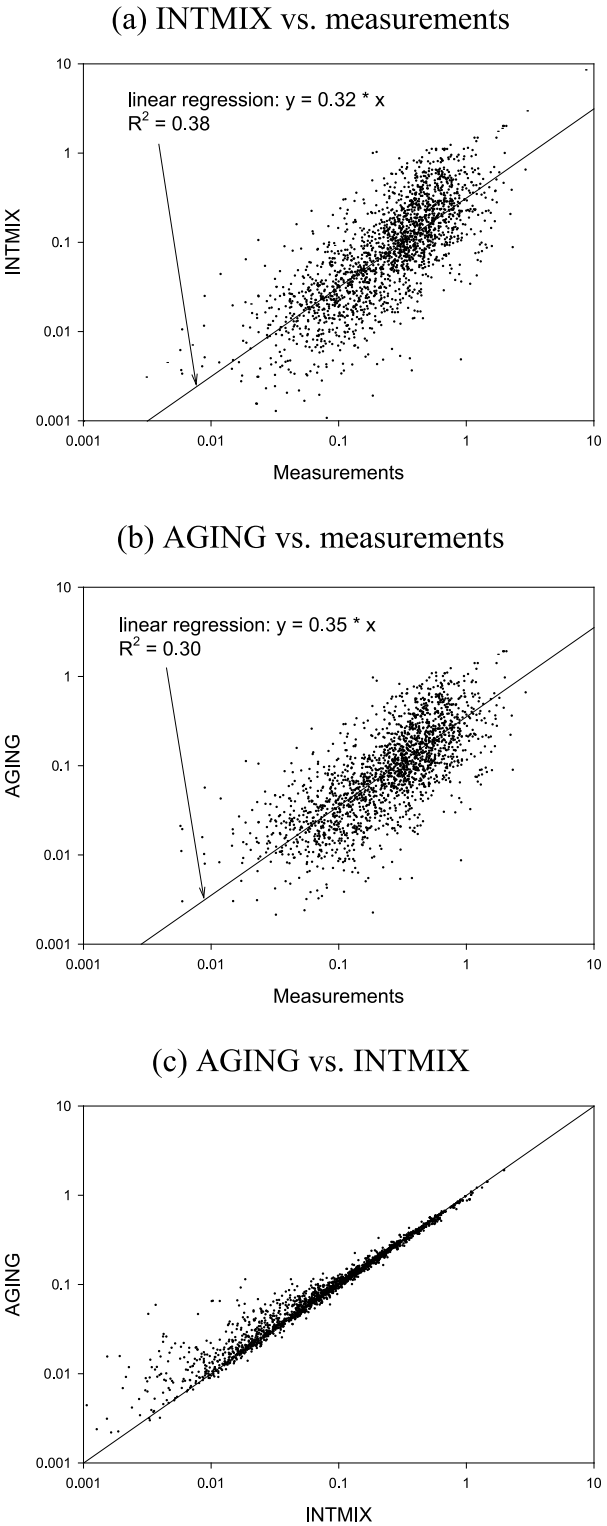

Fig. 2. Model-measurement and inter-model comparisons of $BC_{2.5}$ (μg m^{-3}): (a) INTMIX scenario versus measurements; (b) AGING scenario versus measurements and (c) AGING versus INTMIX.

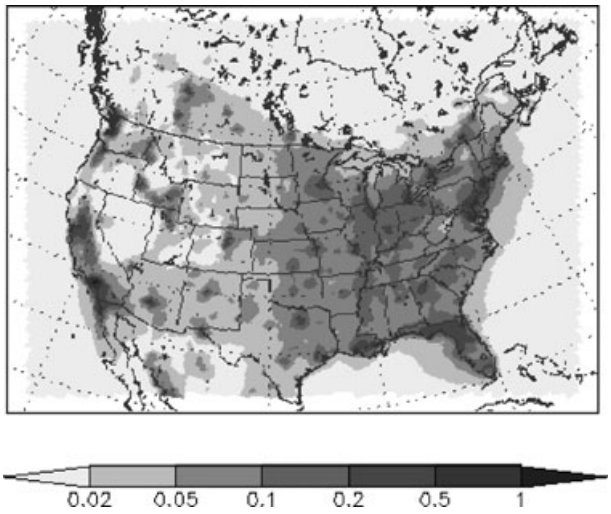

Fig. 3. Concentration of surface $BC_{2.5}$ (μg m^{-3}) predicted by INTMIX scenario.

the two scenarios. It can be seen that $BC_{2.5}$ concentrations predicted by AGING were quite often lower than those predicted by INTMIX, especially in regions where $BC_{2.5}$ concentration is high. This was not expected because internally mixed BC particles can be removed from the atmosphere by wet deposition more easily than externally mixed ones as will be discussed in Section 3.2. The reason for this seemingly contradictory result is discussed below.

Figure 3 shows the mean monthly $BC_{2.5}$ ground-level concentration field (μg m^{-3}) predicted by the original version (INTMIX). BC emissions are associated with combustion processes, including stationary and mobile anthropogenic sources and biomass burning. As already noted, BC emissions from wildfires and prescribed burning were not included in the AURAMS CTM emission files. As a consequence the spatial distribution of $BC_{2.5}$ ground-level concentration broadly reflects the North American population distribution as well as the presence of major transportation corridors, and a west-to-east gradient in $BC_{2.5}$ ground-level concentration is evident.

Figure 4 shows the ratios between the model predictions for $BC_{2.5}$. Fig. 4a shows the ratio of the EXTMIX prediction over the AGING prediction, whereas Fig. 4b shows the ratio of the INTMIX prediction over the AGING prediction. Interestingly, although the inclusion of BC aging processes led to reductions in $BC_{2.5}$ in many regions as was expected, $BC_{2.5}$ concentrations increased in some other regions. The EXTMIX and INTMIX

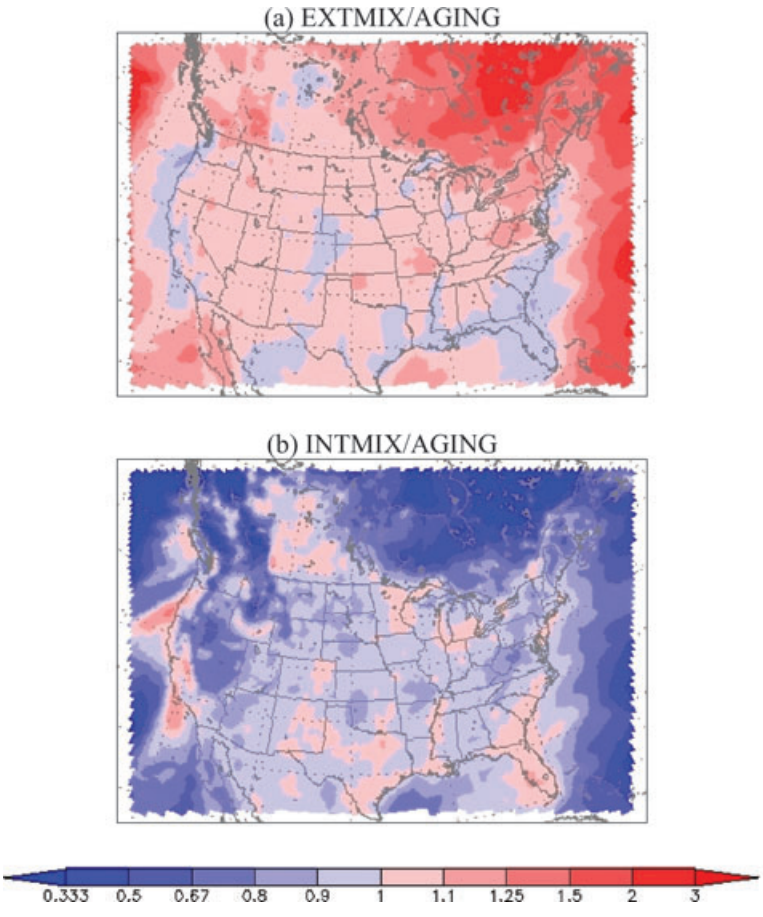

Fig. 4. Ratio of $BC_{2.5}$ monthly concentration (μg m^{-3}) predicted by different scenarios: (a) EXTMIX versus AGING and (b) INTMIX versus AGING.

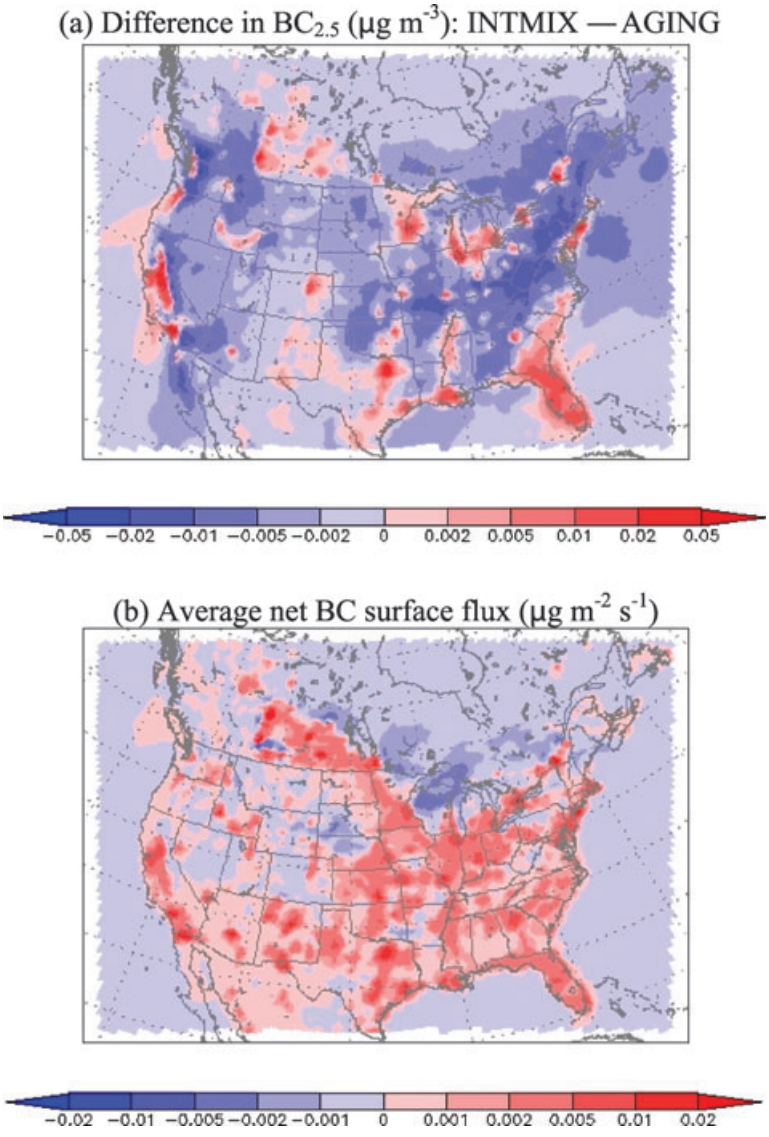

Fig. 5. Comparison of (a) difference in predicted $BC_{2.5}$ for the INTMIX and AGING scenarios to (b) the net BC surface flux for the INTMIX scenario.

model versions seem generally to predict higher and lower $BC_{2.5}$, respectively, compared to the more realistic AGING model version. This overall trend might be expected; EXTMIX preserving the $BC_{2.5}$ for longer periods due to the lack of coagulation and condensation losses, and the INTMIX failing to preserve the unique identity of fresh aerosols, promoting faster growth to larger particle sizes and subsequent losses by settling and deposition. However, at certain locations, this trend was reversed. For example, in Florida, the EXTMIX model version predicted lower $BC_{2.5}$ than AGING, whereas the INTMIX model version predicted higher $BC_{2.5}$ than AGING.

To find out a reason for these seemingly contradictory results, in Fig. 5, the difference in mean monthly ground-level $BC_{2.5}$ concentration predicted by the INTMIX and AGING model versions is compared to the net BC surface flux for the INTMIX model version, which was obtained by subtracting the sum of BC wet and dry deposition from BC emission flux. We can see that many of the dark red spots in these two plots coincide with each other, which indicates that the INTMIX model version predicts considerably higher $BC_{2.5}$ than the AGING model version at strong emission source areas of BC and other species. In these areas, freshly emitted BC particles exist at relatively lower altitudes, so the aging effect on their in-cloud wet removal rate would not be too high. Aging processes will increase the size of particles; depending on their non-aged original sizes, this could either increase or decrease their deposition velocities near the surface. This in turn may lead to higher or lower concentrations close to the surface. Figure 6 was prepared to examine these results further. It shows the vertical distribution of time-averaged BC concentration at a near-source region, Savannah, GA (−81.14, 32.09). At higher elevations above the surface, the INTMIX $BC_{2.5}$ concentration was the lowest of the three simulations

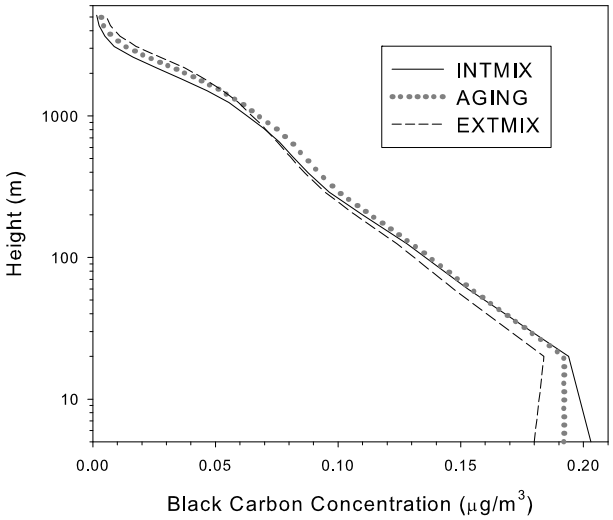

Fig. 6. Vertical distribution of time-averaged BC concentration at a near source region, Savannah, GA (32.09°N, 81.14°W).

because of enhanced in-cloud wet removal rate. On the other hand, near the surface, the INTMIX $BC_{2.5}$ concentration was the highest because of increased shift towards lower removal. EXTMIX will tend to have more particles in the smaller sizes (increasing deposition; to the left of the accumulation mode peak). INTMIX will tend to cause the particles to reach the accumulation mode peak (i.e. the surface deposition minimum) most efficiently of the three simulations, hence has the highest mass just above the surface. AGING, with some un-aged BC retained while also having some aging processes active, lies between the other two simulations. A few more near-source locations were examined and a similar trend was observed.

3.2. Impacts of BC aging on CCN number

Externally mixed BC particles are hydrophobic and hence are not influenced by aerosol-cloud interaction. Changes in the mixing state of BC particles due to aging processes, however, enable them to participate in the CCN activation process (Pierce et al., 2007). One can refer to Gong et al. (2003) for the aerosol activation scheme employed in AURAMS. Figure 7 compares the average CCN-number column loading (m^{-2}) predicted for the three different mixing-state scenarios. It is evident that relative to the EXTMIX scenario, CCN number is increased significantly by aging processes and that the internal-mixture assumption (INTMIX) leads to a considerably larger estimation of the CCN concentration than the AGING scenario.

Aged particles that activate as cloud nuclei can be removed by in-cloud wet removal processes, which is not the case for fresh, externally mixed hydrophobic particles. The accumulated BC wet deposition (kg) over the whole model domain predicted for the three different scenarios are compared in Table 2. Time-averaged CCN number and BC mass burdens (i.e. total

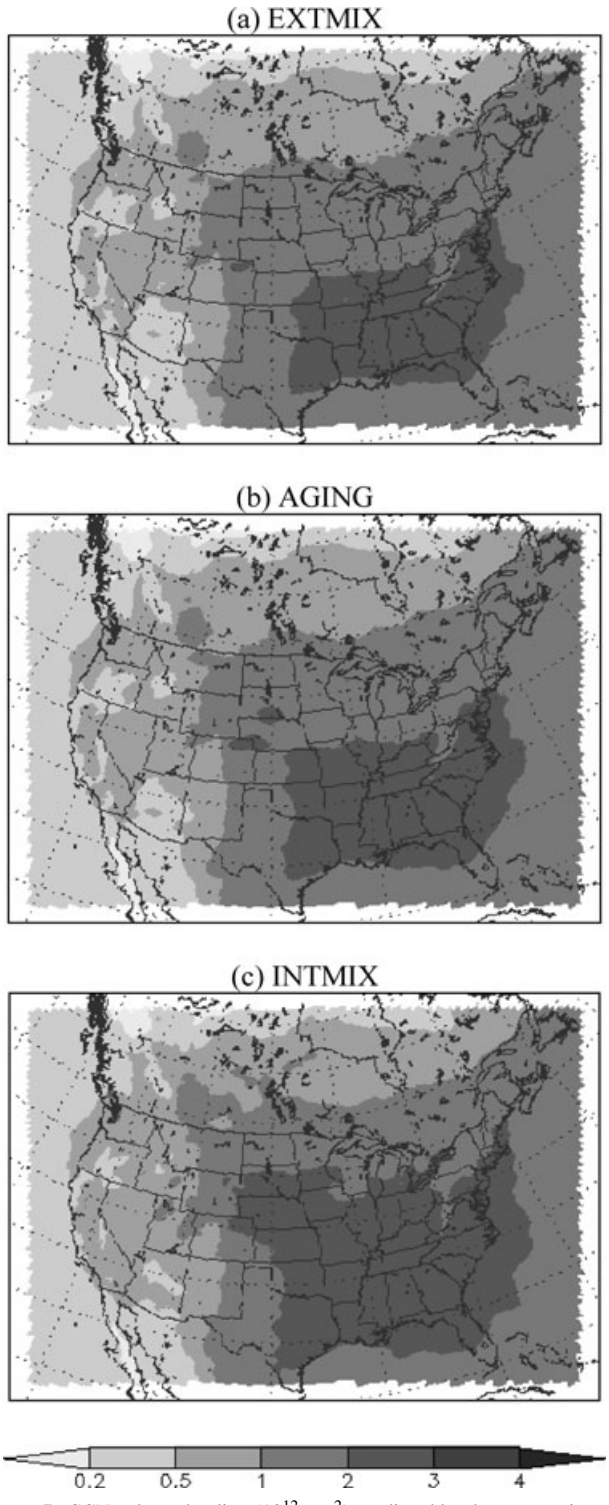

Fig. 7. CCN column loading (10^{12} m^{-2}) predicted by three scenarios: (a) EXTMIX; (b) AGING and (c) INTMIX.

Table 2. Accumulated wet deposition and time-averaged CCN number and BC mass burdens over the whole model domain predicted by three different scenarios for April 2002. Relative fractions of the EXTMIX and INTMIX scenarios versus 1 for the AGING scenario are shown in parenthesis

	EXTMIX	AGING	INTMIX
Time-averaged CCN number burden	3.1×10^{25} (0.96)	3.3×10^{25}	3.5×10^{25} (1.08)
Accumulated wet deposition (kg)	2.2×10^{7} (0.86)	2.5×10^{7}	2.9×10^{7} (1.13)
Time-averaged BC mass burden (Gg)	5.2 (1.17)	4.5	3.5 (0.78)

atmospheric CCN number and BC mass) over the whole model domain are shown together in this table. Relative fractions of the EXTMIX and INTMIX scenarios versus 1 for the AGING scenario are also shown for each of these three quantities. Similar to CCN burden, the amount of wet deposition increased due to aging for the AGING scenario (by 14%) but was less than for the INTMIX scenario (by 13%).

CCN activation and consequent in-cloud removal of BC particles due to aging may reduce their atmospheric lifetime significantly. Figure 8 compares the BC mass column loading predicted for the three different scenarios. BC mass column loading is shown to decrease as a result of aging as was expected. The fraction of internally mixed (aged) BC in the total BC mass column loading of the AGING scenario is shown in Fig. 9. It can be seen that BC particles over the continent are mainly externally mixed. Only over two downwind locations (see the wind field shown in Fig. 1) over the ocean, one at the southwestern corner of the model domain west of Baja California and the other over the Atlantic Ocean east of the high-SO_2-emissions Ohio Valley region, the amount of internally mixed BC was comparable to the amount of externally mixed BC. The low fraction of internally mixed BC over the continent and higher fraction over the oceans downwind predicted by our model is consistent with available observations. For example, Hasegawa and Ohta (2002) investigated the mixing state of soot-containing particles in Japan and reported that the number fractions of internally mixed soot particles were 19–72% and 56% at two remote areas, whereas only 5–7% were observed to be internally mixed in an urban area. In an industrialized region in France, most BC was found to be externally mixed (Mallet et al., 2004). It should be noted, however, that much higher fraction of internally mixed BC has been reported in the literature for certain remote areas. Posfai et al. (1999) observed that more than 93% of BC-containing particles contained sulphate over the North Atlantic. It was also reported that 85% of BC in accumulation mode was internally mixed in Asian outflow (Clarke et al., 2004). The extremely

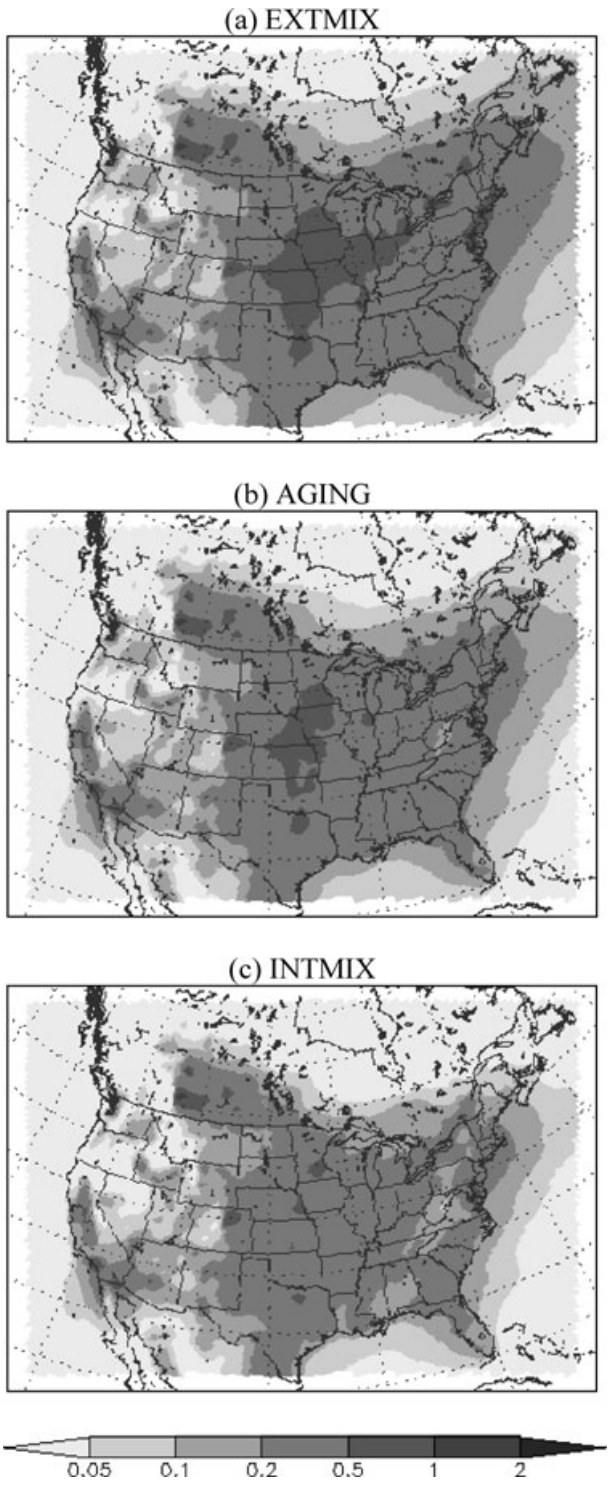

Fig. 8. BC mass column loading (mg m^{-2}) predicted by three scenarios: (a) EXTMIX; (b) AGING and (c) INTMIX.

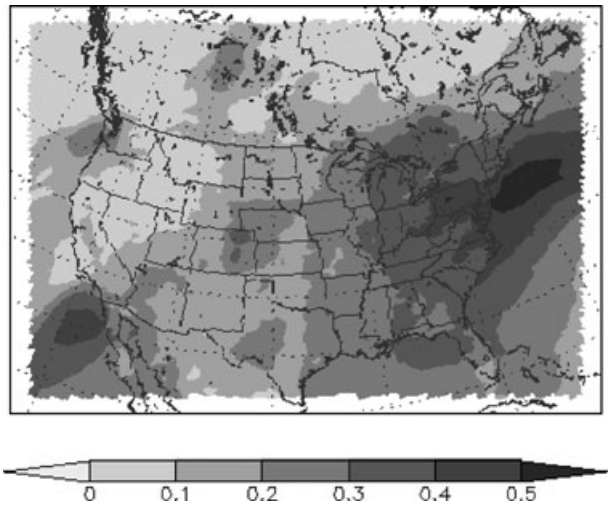

Fig. 9. Fraction of internally mixed BC in total BC mass column loading for the AGING scenario.

high fraction of internally mixed BC in these two regions seems to stem from their particular location. The particles over North Atlantic had been transported much farther from their source region and hence had more opportunities to be aged than the particles over any area included in the current spatial domain. Particles entrained in Asian outflow may had been affected by very high sulphate concentration leading to rapid aging due to the active industrial development in East Asia region. Moffet and Prather (2009) reported that the aging time scale of BC was very short, about 3 h, in urban areas. That result agrees with the computation of this study: the aging time scale of BC is shown to be less than 10 h in several urban areas within the spatial domain of this study (Fig. 10a). Except over these particular urban areas, located mostly in eastern North America, the aging time scale is shown to be much higher explaining a reason of relatively low fraction of internally mixed BC predicted in this study. It should also be noted that the neglect of the role of secondary organic species via both coagulation and condensation may have contributed partially to somewhat lower fraction of internally mixed BC in this study. Our results here suggest that the time scale to reach significant levels of internal mixing may be large enough that external mixing may be the norm over continental areas.

3.3. Implications for climate forcing

Although this study was aimed mainly at investigating the influence of BC aging on North American AQ, it is worth discussing the climate impacts of BC aging based on the information obtained in this study.

The direct radiative forcing (DRF) of BC in the spatial and temporal domain of this study can be estimated roughly from the average BC burden. Chylek and Wong (1995) derived the

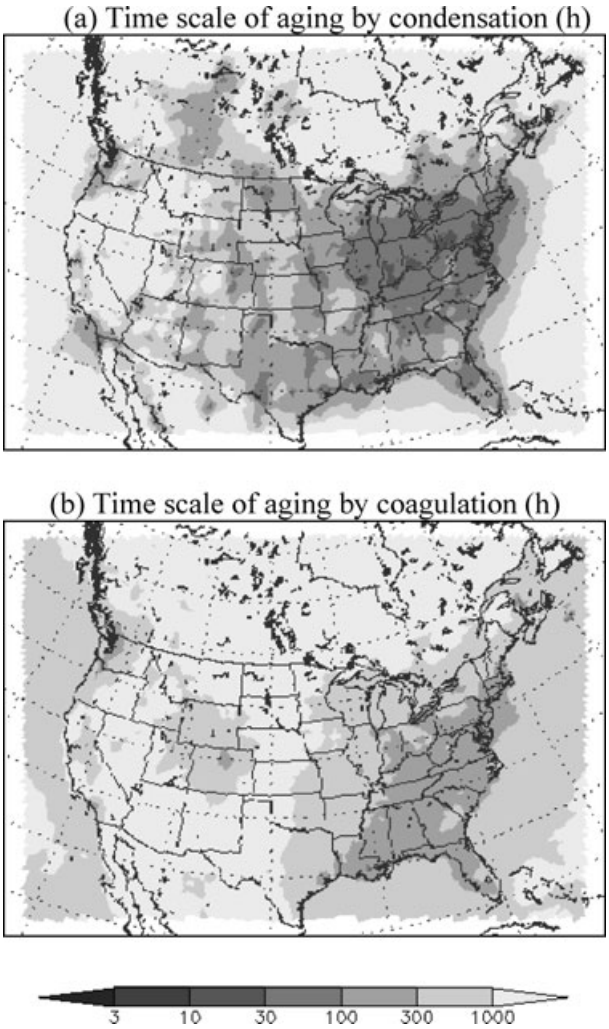

Fig. 10. Time scales of aging (h) by (a) sulphate condensation and (b) coagulation for the AGING scenario.

following equation from the radiation transfer equation:

$$\mathrm{DRF} = \frac{S_0}{4} T_{\mathrm{atm}}^2 (1 - F_c) \left\{ 4a\delta_{ab} - 2(1-a)^2 \beta \delta_{sc} \right\}, \tag{7}$$

where S_0 is the solar irradiance, T_{atm} is the atmospheric transmission, F_c is the cloud fraction, a is the surface albedo, δ_{ab} is the absorption optical depth, β is the back-scattering fraction and δ_{sc} is the scattering optical depth. The optical depths can be obtained by

$$\delta = \sum_{n=1}^{N_L} c_n \sigma_n \Delta H_n, \tag{8}$$

where N_L is the number of vertical layers, c_n is the BC mass concentration at the nth vertical layer, σ_n is the specific cross-section and ΔH_n is the thickness of the nth vertical layer.

The input parameters required in Eqs. (7) and (8) were suggested by Bond and Bergstrom (2006) as follows:

Table 3. Land-cover categories used in AURAMS and corresponding surface albedo.

Category	Description	Surface albedo
1	Evergreen needleleaf trees	0.12
2	Evergreen broadleaf trees	0.12
3	Deciduous needleleaf trees	0.14
4	Deciduous broadleaf trees	0.16
5	Mixed broadleaf and needleleaf trees	0.13
6	Grass	0.19
7	Crops, mixed farming	0.18
8	Desert	0.25
9	Tundra	0.15
10	Shrubs and interrupted woodlands	0.22
11	Wet land with plants	0.14
12	Ice cap and glacier	0.55
13	Inland water	0.08
14	Ocean	0.08
15	Urban	0.15

Specific absorption cross-section basically depends on particle size, but is almost constant for spherical particles less than about 100 nm. For aggregate particles, the total absorption is assumed to be the sum of absorption by each primary particle. In many circumstances, BC particles are aggregates of primary particles smaller than 100 nm. Therefore, a constant value of 7500 ± 1.2 m^2 kg^{-1} can be used.

Mixing state effect factor is the enhancement of absorption by the change in mixing state from external mixture to internal mixture due to aging. This factor was estimated to be two by global simulations of Jacobson (2000) and (2001). Bond et al. (2006) suggested a lower value of about 1.5 taking into account the effect of destruction of the aggregate structure due to aging. In the DRF calculations shown below, both 1.5 and 2 are used and the results are compared.

Single scattering albedo is assumed to be 0.25 ± 0.05 for fresh BC aerosols, which translates into *Specific scattering cross-section* of 2500 m^2 kg^{-1}.

Back-scattering fraction is assumed to be 0.17 ± 0.01.

The cloud cover was assumed to be 0.6 and the surface albedo was decided according to the dominant land-cover category of each surface grid as shown in Table 3.

In this study, the average BC DRF over the spatial domain used was computed using Eqs. (7) and (8) separately for three scenarios: EXTMIX; AGING and INTMIX. The total BC burdens for three scenarios were 5.2, 4.5 and 3.5 Gg, respectively, as was shown in Table 2. The average percentage of internally mixed BC in AGING scenario was 24%. This is much lower than the global average reported by Jacobson (2001), which indicates that the spherical-particle assumption did not impose a very adverse influence on the simulation results, but agrees with observations taken over continental source regions as discussed above.

The average DRF calculated for EXTMIX, AGING and INTMIX were 0.064, 0.069 and 0.092 W m^{-2}, respectively when the mixing state effect factor was set at two. The assumption of an internal mixture, which is used in the current version of AURAMS, would thus lead to a 32% higher estimate on average of BC DRF over North America, relative to the AGING case. This result gives an insight for possible bias for the estimation of BC DRF by global modelling. Due to the computational cost, some global climate models with detailed aerosol dynamics assumes the internal mixing state of aerosol particles (e.g. Pierce et al. (2007) and Spracklen et al. (2006)), which may lead to overestimation of BC DRF as the current AURAMS version (INTMIX) did. Gradual aging due to aerosol dynamics processes needs to be adapted in global models for more accurate estimation of BC DRF, which has never been done yet.

The ratio of direct forcing of an internal mixture over that of an external mixture is 1.43, which is much smaller than 2, the mixing state effect factor. This ratio stems mainly from the differences between the following properties of BC particles in the two scenarios: absorbance depending on mixing state, wet deposition rate depending on hygroscopicity and dry deposition rate depending on size distribution. When we compared the rates of wet and dry depositions, the rate of dry deposition was much smaller than that of wet deposition for the spatial and temporal domain simulated in this study. Moreover, the change in dry deposition rate due to coagulation that alters particle size distribution is only a small part of total dry deposition rate. This indicates that the change in dry deposition rate due to aging was not significant in this study and that the above-mentioned ratio of 1.43 can be regarded as a combined result of the mixing state effect and enhanced wet removal only. If only aging is considered without accounting for increase in wet removal, and hence decreased BC burden, the factor will be the same as the mixing state effect factor, by definition. Therefore, one can conclude that the effect of increased wet deposition of BC due to aging partially compensated for the effect of increased absorbance.

Another impact of enhanced absorption due to aging is corresponding reduction of scattering. It is not easy to quantify, however, how large reduction in scattering would be resulted due to enhanced absorption. Therefore, a simple sensitivity test with a change in scattering cross-section is provided here. When the specific scattering cross-section was set at 2000 m^2 kg^{-1} instead of 2500 m^2 kg^{-1} for AGING scenario, the average DRF was calculated to be 0.071 W m^{-2}, with an increase of 0.002 W m^{-2}.

Another set of simulations were carried out with the mixing state effect factor set at 1.5. The average DRF calculated for EXTMIX, AGING and INTMIX were 0.064, 0.063 and 0.069 W m^{-2}, respectively. The ratio of direct forcing of an internal mixture over that of an external mixture is even smaller,

1.07, which indicates that the effect of increased absorbance due to aging has been almost completely compensated by the effects of increased wet deposition and loss of aggregate structure. If the aggregate structure is partially destroyed due to aging, the reality would exist between the above two cases, that is, the mixing state effect factors of 2 and 1.5. The results of the present simulations suggest that the overall effect of aging on BC direct radiative forcing may be much less significant than is implied by the mixing state effect factor.

The increase of CCN concentration due to BC aging imposes additional climate impacts of BC via the indirect effect due to the changes in the cloud amount and albedo, which adds a negative forcing. The semidirect effect due to heating in the clouds, resulting in a positive forcing, is also important. BC existing between or within cloud drops absorbs sunlight warming the cloud, reducing the cloud amount and enhancing stability (Hansen et al., 1997; Ackerman et al., 2000; Jacobson, 2006, 2010). This effect is of particular importance when BC particles in cloud are treated as aggregates consisting of polydisperse spherical primaries rather than just a single large core (Jacobson, 2006). It is not possible to quantify the indirect and semidirect effects of a single atmospheric component because all those effects of all components are linked together, so that one cannot change only one component while keeping the others constant. Nevertheless, Jacobson (2002) tried to obtain a qualitative physical insight into the indirect and semidirect effects of BC using a global simulation study. Under the internal-mixture (with a BC core) assumption, he found that the cloud-scattering optical depth increased and the average cloud size decreased due to emissions of BC, which indicated that the net indirect and semidirect effects of BC were negative. When these effects are also included, the ratio of climate forcing of internal mixture over that of external mixture will be even less than the values obtained in this study. The result of this study indicates that changes in the hygroscopic properties of BC due to aging and correspondingly the BC total burden must be taken into account to quantify the impacts of BC aging on climate.

In this study, the direct radiative forcing of BC particles and the effect of aging on it were calculated using a simple parameterization for direct forcing which may give results different from a spectral radiative transfer code used in 3-D models. Therefore, the readers should be careful when comparing the results of this study with results from 3-D models. It must also be pointed out that there are other processes not taken into account in the parameterization that affect climate forcing of BC particles. More precise quantification is possible only by thorough modelling accounting for all those processes, which is beyond the scope of this study.

In climate modelling, the BC aging process is often not solved in detail but is parameterized using an aging time scale to reduce the computing time. The rate of aging can be represented by a characteristic aging time scale. Eqs. (1) and (5) can each be written in the form

$$\frac{\mathrm{d}x_i}{\mathrm{d}t} = -\frac{Q_i}{S_i} \cdot x_i = -\frac{x_i}{\tau_i}, \tag{9}$$

where τ_i $(= S_i/Q_i)$ is the characteristic aging time scale for size section i at a given grid cell. The column-averaged characteristic time scale of aging for all BC particles over the whole simulation time period can then be computed by the expression

$$\bar{\tau} = \frac{\int_z \int_t \sum_i x_i \, dt dz}{\int_z \int_t \sum_i \frac{x_i}{\tau_i} dt dz}, \tag{10}$$

where z is the vertical coordinate variable.

Figure 10 shows the column-averaged characteristic aging time scale for condensation and for coagulation obtained from the 1-month simulation for April 2002 using the AGING model version. The aging of BC seems to be dominated by condensation except over the sea, where the coagulation with sea-salt particles is more important. As expected, the spatial variation of the characteristic aging time scale for condensation is closely linked to the spatial distribution of particle sulphate (not shown).

4. Conclusions

In this study, the effect of aging on the distribution of BC over North America was investigated using the AURAMS regional AQ model. Over the domain studied here, BC aging was dominated by sulphate condensation except over the ocean. CCN number was shown to be increased significantly by aging processes and the internal-mixture assumption led to a considerable overestimation of the CCN number concentration. Accordingly, the amount of BC wet deposition increased and BC mass column loading decreased as a result of aging. The ground level BC concentration in $PM_{2.5,}$ however, was predicted to increase due to aging near BC source regions, where the aging effect is not too high. The vertical distribution of BC suggested that this result can be attributed to changes in the particle size, hence removal rate, due to aging. With the gradual aging process incorporated into the model, the comparison with ground-level BC concentration observations from the 1-month simulation period (April 2002) was slightly improved although the difference was not statistically significant.

Based on the simulation results, for the three BC mixing-state assumptions of external mixture, gradual aging and internal mixture, the domain-average BC direct radiative forcing was estimated to be 0.064, 0.069 and 0.092 W m^{-2}, respectively, when the mixing state effect factor was set at two. The ratio of direct forcing of an internal mixture over that of an external mixture predicted in this study was much smaller than the mixing state effect factor. The effect of increased wet deposition and hence decreased burden of BC due to aging compensated, at least partially, for the effect of increased absorbance. If the destruction of aggregate structure by aging is accounted for, the

BC absorption enhancement can drop further, which suggests that the overall effect of aging on BC direct radiative forcing may be much less significant than is implied by the mixing state effect factor. Therefore, the changes in the hygroscopicity of BC due to aging and the accompanying change in total BC burden must be taken into account to quantify the impact of BC aging on climate accurately.

Our analysis is subject to a few limitations worthy of mention; specifically the use of a single monolayer of sulphate as a criterion for condensational aging, and the use of 5% as a similar cutoff to define aging through coagulation. While these criteria are of necessity simple, they are not wholly arbitrary. The monolayer criterion stems from the simple understanding that to the outside world, the coated particle at that point appears to be entirely sulphate. Similarly, the 5% mass criterion for soluble material for coagulation is made under the assumption that amount should be sufficient to coat the coagulated, 'new' particle with a layer of soluble material. We note that their use has improved the model's ability to simulate BC, and that modification of these limits under controlled conditions in future simulations may result in further improvements to the simulation results. It should also be noted that the direct radiative forcing results of this study were obtained with a simplified parameterization, which may give results different from a spectral radiative transfer code used in 3-D models. Therefore, the readers should be careful when comparing the results of this study with results from 3-D models.

Acknowledgments

The authors acknowledge the Environment Canada National Atmospheric Chemistry database and its data-contributing agencies/organizations, including the U.S. Environmental Protection Agency Air Quality System and Interagency Monitoring of Protected Visual Environments network for the provision of the measurement data used in this paper. This work was supported by the Korea Research Foundation Grant funded by the Korean Government (KRF-2008–331-D00279), in which main calculations were performed by using the supercomputing resource of the Korea Institute of Science and Technology Information (KISTI), and by PERD (Program of Energy Research and Development). Authors also wish to acknowledge the support by the Chinese National Basic Research Program (Project No. 2011CB403404).

References

Ackerman, A. S., Toon, O. B., Stevens, D. E., Heymsfield, A. J., Ramanathan, V., and co-authors. 2000. Reduction of tropical cloudiness by soot. *Science* **288**, 1042–1047.

Ackerman, T. P., and Toon, O. B. 1981. Absorption of visible radiation in atmosphere containing mixtures of absorbing and non-absorbing particles. *Appl. Opt.* **20**, 3661–3668.

Bond, T. C., and Bergstrom, R. W. 2006. Light absorption by carbonaceous particles: an investigative review. *Aerosol Sci. Technol.* **40**, 27–67.

Bond, T. C., Habib, G., and Bergstrom, R. W. 2006. Limitations in the enhancement of visible light absorption due to mixing state. *J. Geophys. Res.* **111**, D20211, doi:20210.21029/22006JD007315.

Chow, J. C., Watson, J. G., Chen, L. W. A., Arnott, W. P., Moosmuller, H., and co-authors. 2004. Equivalence of elemental carbon by thermal/optical reflectance and transmittance with different temperature protocols. *Environ. Sci. Technol.* **38**, 4414–4422.

Chu, S.-H. 2004. PM2.5 episodes as observed in the speciation trends network. *Atmos. Environ.* **38**, 5237–5246.

Chylek, P., and Wong, J. 1995. Effect of absorbing aerosols on global radiation budget. *Geophys. Res. Lett.* **22**, 929–931.

Clarke, A. D., Shinozuka, Y., Kapustin, V. N., Howell, S., Huebert, B., and co-authors. 2004. Size distributions and mixtures of dust and black carbon aerosol in Asian outflow: physiochemistry and optical properties. *J. Geophys. Res.* **109**, D15S09, doi:10.1029/2003JD004378.

Croft, B., Lohmann, U., and von Salzen, K. 2005. Black carbon ageing in the Canadian Centre for Climate modelling and analysis atmospheric general circulation model. *Atmos. Chem. Phys.* **5**, 1931–1949.

Dasenbrock, C., Peters, L., Creutzenberg, O., and Heinrich, U. 1996. The carcinogenic potency of carbon particles with and without PAH after repeated intratracheal administration in the rat. *Toxicol. Lett.* **88**, 15–21.

Devore, J. L. 1982. *Probability & Statistics for Engineering and the Sciences*. Brooks/Cole Publishing Company, Monterey, CA.

Ech, T. F., Holben, B. N., Slutsker, I., and Setzer, A. 1998. Measurements of irradiance attenuation and estimation of the aerosol single scattering albedo for biomass burning in Amazonia. *J. Geophys. Res.* **103**, 31 865–31 878.

Fuchs, N. A., and Sutugin, A. G. 1971. High-dispersed aerosols. In: *Topics in Current Aerosol Research*, (eds. G. M. Hidy and J. R. Brock). Pergamon Press, New York, 1–60.

Gego, E. L., Porter, P. S., Irwin, J. S., Hogrefe, C., and Rao, S. T. 2005. Assessing the comparability of ammonium, nitrate, and sulfate concentrations measured by three air quality monitoring networks. *Pure Appl. Geophys.* **162**, 1919–1939.

Gong, S. L., Barrie, L. A., Blanchet, J.-P., Salzen, K. v., Lohmann, U., and co-authors. 2003. Canadian Aerosol Module: a size-segregated simulation of atmospheric aerosol processes for climate and air quality models 1. Module development. *J. Geophys. Res.* **108**, 4007, doi:4010.1029/2001JD002002.

Gong, W., Dastoor, A. P., Bouchet, V. S., Gong, S., Makar, P. A., and co-authors. 2006. Cloud processing of gases and aerosols in a regional air quality model (AURAMS). *Atmos. Res.* **82**, 248–275.

Hansen, J., Sato, M., and Ruedy, R. 1997. Radiative forcing and climate response. *J. Geophys. Res.* **102**, 6831–6864.

Hasegawa, S., and Ohta, S. 2002. Some measurements of the mixing state of soot-containing particles at urban and nonurban sites. *Atmos. Environ.* **36**, 3899–3908.

Haywood, J., and Boucher, O. 2000. Estimates of the direct and indirect radiative forcing due to tropospheric aerosols. *Rev. Geophys.* **38**, 513–543.

IPCC. 2007. *Climate Change 2007: The Physical Science Basis: Contribution of Working Group I to the Fourth Assessment Report of the Intergovernmental Panel on Climate Change*, (eds. S. Solomon, D. Qin, M. Manning, Z. Chen, M. Marquis, K. B. Averyt, M. Tignor, and H. L. Miller). Cambridge University Press, Cambridge, United Kingdom and New York, NY, USA.

Jacobson, M. C. 2002. Control of fossil-fuel particulate black carbon and organic matter, possibly the most effective method of slowing global warming. *J. Geophys. Res.* **107**, 4410, doi:4410.1029/2001JD001376.

Jacobson, M. Z. 1997. Development and application of a new air pollution modeling system. Part III: aerosol-phase simulations. *Atmos. Environ.* **31**, 587–608.

Jacobson, M. Z. 2000. A physically-based treatment of elemental carbon optics: implications for global direct forcing of aerosols. *Geophys. Res. Lett.* **27**, 217–220.

Jacobson, M. Z. 2001. Strong radiative heating due to the mixing state of black carbon in atmospheric aerosols. *Nature* **409**, 695–697.

Jacobson, M. Z. 2006. Effects of absorption by soot inclusions within clouds and precipitation on global climate. *J. Phys. Chem.* **110**, 6860–6873.

Jacobson, M. Z. 2010. Short-term effects of controlling fossil-fuel soot, biofuel soot and gases, and methane on climate, arctic ice, and air pollution health. *J. Geophys. Res.* **115**, D14209, doi:14210.11029/12009JD013795.

Jacobson, M. Z., Kaufmann, Y. J., and Rudich, Y. 2007. Examining feedbacks of aerosols to urban climate with a model that treats 3-D clouds with aerosol inclusions. *J. Geophys. Res.* **112**, D24205, doi:24210.21029/22007JD008922.

Jacobson, M. Z., Turco, R. P., Jensen, E. J., and Toon, O. B. 1994. Modeling coagulation among particles of different composition and size. *Atmos. Environ.* **28**, 1327–1338.

Lesins, G., Chylek, P., and Lohmann, U. 2002. A study of internal and external mixing scenarios and its effect on aerosol optical properties and direct radiative forcing. *J. Geophys. Res.* **107**, 4094, doi:4010.1029/2001JD000973.

Liu, X., Penner, J. E., and Herzog, M. 2005. Global modeling of aerosol dynamics: model description, evaluation, and interactions between sulfate and nonsulfate aerosols. *J. Geophys. Res.* **110**, D18206, doi:18210.11029/12004JD005674.

Mallet, M., Roger, J. C., Despiau, S., Putaud, J. P., and Dubovik, O. 2004. A study of the mixing state of black carbon in urban zone. *J. Geophys. Res.* **109**, D04202, doi:04210.01029/02003JD003940.

Malm, W. C., Sisler, J. F., Huffman, D., Eldred, R. A., and Cahill, T. A. 1994. Spatial and seasonal trends in particle concentration and optical extinction in the United States. *J. Geophys. Res.* **99**, 1347–1370.

Martins, J. V., Artaxo, P., Liousse, C., Reid, J. S., Hobbs, P. V., and co-authors. 1998. Effects of black carbon content, particle size, and mixing on light absorption by aerosol particles from biomass burning in Brazil. *J. Geophys. Res.* **103**, 32 041–32 050.

Menon, S., Hansen, J., Nazarenko, L., and Luo, Y. 2002. Climate effects of Black Carbon aerosols in China and India. *Science* **297**, 2250–2253.

Moffet, R. C., and Prather, K. A. 2009. In-situ measurements of the mixing state and optical properties of soot with implications for radiative forcing estimates. *Proc. Natl. Acad. Sci. U. S. A.* **106**, 11 872–11 877.

Oshima, N., Koike, M., Zhang, Y., Kondo, Y., Moteki, N., and co-authors. 2009. Aging of black carbon in outflow from anthropogenic sources using a mixing state resolved model: model development and evaluation. *J. Geophys. Res.* **114**, D06210, doi:06210.01029/02008JD010680.

Park, S. H., Gong, S. L., Zhao, T. L., Vet, R. J., Bouchet, V. S., and co-authors. 2007. Simulation of entrainment and transport of dust particles within North America in April 2001 ("Red Dust Episode"). *J. Geophys. Res.* **112**, D20209, doi:20210.21029/22007JD008443.

Phillips, S. B., and Finkelstein, P. L. 2006. Comparison of spatial patterns of pollutant distribution with CMAQ predictions. *Atmos. Environ.* **40**, 4999–5009.

Pierce, J. R., Chen, K., and Adams, P. J. 2007. Contribution of primary carbonaceous aerosol to cloud condensation nuclei: processes and uncertainties evaluated with a global aerosol microphysics model. *Atmos. Chem. Phys.* **7**, 5447–5466.

Posfai, M., Anderson, J. R., Buseck, P. R., and Sievering, H. 1999. Soot and sulfate aerosol particles in the remote marine troposphere. *J. Geophys. Res.* **104**, 21 685–21 693.

Ramanathan, V., and Carmichael, G. 2008. Global and regional climate changes due to black carbon. *Nat. Geosci.* **1**, 221–227.

Riemer, N., West, M., Zaveri, R., and Easter, R. 2010. Estimating black carbon aging time-scales with a particle-resolved aerosol model. *J. Aerosol Sci.* **41**, 143–158.

Riemer, N., West, M., Zaveri, R. A., and Easter, R. C. 2009. Simulating the evolution of soot mixing state with a particle-resolved aerosol model. *J. Geophys. Res.* **114**, D09202, doi:09210.01029/02008JD011073.

Saathoff, H., Naumann, K. H., Schnaiter, M., Schock, W., Mohler, O., and co-authors. 2003. Coating of soot and (NH4)2SO4 particles by ozonolysis products of -pinene. *J. Aerosol Sci.* **34**, 1297–1321.

Samaali, M., Moran, M. D., Bouchet, V. S., Pavlovic, R., Cousineau, S., and co-authors. 2009. On the influence of chemical initial and boundary conditions on annual regional air quality model simulations for North America. *Atmos. Environ.* **43**, 4873–4885.

Satheesh, S. K., and Ramanathan, V. 2000. Large differences in tropical aerosol forcing at the top of the atmosphere and Earth's surface. *Nature* **405**, 60–63.

Spracklen, D. V., Carslaw, K. S., Kulmala, M., Kerminen, V. M., Mann, G. W., and co-authors. 2006. The contribution of boundary layer nucleation events to total particle concentrations on regional and global scales. *Atmos. Chem. Phys.* **6**, 5631–5648.

Vignati, E., Karl, M., Krol, M., Wilson, J., Stier, P., and co-authors. 2010. Sources of uncertainties in modelling black carbon at the global scale. *Atmos. Chem. Phys.* **10**, 2595–2611.

Vignati, E., Wilson, J., and Stier, P. 2004. M7: an efficient size-resolved aerosol microphysics module for large-scale aerosol transport models. *J. Geophys. Res.* **109**, D22202, doi:22210.21029/22003JD004485.

Vogel, B. 2009. The interactions of aerosols, clouds and radiation on the regional to the continental scale simulated with COSMO-ART. Paper presented at: International Aerosol Modeling Algorithms Conference (Davis, California).

Zaveri, R., Easter, R. C., Barnard, J. C., Riemer, N., and West, M. 2009. Evaluating the effects of mixing state assumptions in aerosol modules on the predicted optical and CCN activation properties. Paper presented at: International Aerosol Modeling Algorithms Conference (Davis, California).

Zhang, L., Gong, S., Padro, J., and Barrie, L. 2001. A size-segregated particle dry deposition scheme for an atmospheric aerosol module. *Atmos. Environ.* **35**, 549–560.

Zhang, L., Moran, M. D., Makar, P. A., Brook, J. R., and Gong, S. 2002. Modelling gaseous dry deposition in AURAMS – A Unified Regional Air-quality Modelling System. *Atmos. Environ.* **36**, 537–560.